Direct band Ge photoluminescence near 1.6 μm coupled to Ge-on-Si microdisk resonators

Gary Shambat,[1,a)] Szu-Lin Cheng,[2] Jesse Lu,[1] Yoshio Nishi,[1] and Jelena Vuckovic[1]
[1]*Department of Electrical Engineering, Stanford University, Stanford, California 94305-4085, USA*
[2]*Department of Materials Science and Engineering, Stanford University, Stanford, California 94305-4085, USA*

(Received 16 September 2010; accepted 22 November 2010; published online 13 December 2010)

We fabricate and optically characterize germanium microdisks formed out of epitaxial germanium grown on silicon. Resonators coupled to fiber tapers display clear whispering gallery modes in transmission and photoluminescence with quality factors limited by germanium's material absorption. Continuous wave pumping of the cavities resulted in a dominant heating effect for the cavity modes in both transmission and photoluminescence. Pulsed optical pumping proved to be more effective in minimizing heating, but was not sufficient to observe material gain or lasing. We believe that significantly higher doping levels are critical in order to achieve lasing at reasonable pump conditions. © *2010 American Institute of Physics*. [doi:10.1063/1.3526732]

Germanium has recently attracted much attention as a complementary metal-oxide semiconductor compatible optical material that can be easily integrated on-chip. Ordinary bulk germanium has poor emission behavior due to its indirect bandgap, positioned approximately 0.136 eV below its direct bandgap. Strategies to improve the luminescence properties of germanium have included tensile strain,[1] tin alloying,[2] quantum confinement,[3] and electron band filling.[4] We focus on the last approach since the emission wavelength for such materials is near the desired telecom-band of 1.55 μm. Previously, there have been several reports on the photoluminescence (PL) and electroluminescence properties of doped germanium, demonstrating the effectiveness of heavy n-type doping on emission.[5–7] Recently, Liu *et al.*[8] showed an optically pumped germanium-on-silicon laser utilizing a large Fabry–Perot cavity structure. For optical emitters on-chip, it would be preferable to scale down the cavity size to the micron-scale for dense integration. Microdisk resonators, for example, have the advantages of a small footprint and a high quality (Q) factor that allow for low threshold lasing with reduced power consumption. Furthermore, microdisks can be efficiently coupled to output waveguides for routing light on-chip and can be easily electrically contacted. In this work we study the behavior of light emission from germanium microdisk cavities grown on silicon substrates under various optical pumping conditions.

Microdisk resonators were formed by depositing 1 μm of germanium-on-silicon substrates in a chemical vapor deposition reactor with multiple deposition and annealing steps.[5] n-type samples were doped *in situ* by flowing phosphine gas during the deposition and were limited to 1×10^{19} cm^{-3} doping levels to avoid reduced crystal quality at higher levels. Disks were defined using optical lithography and dry etching before undercutting the Si sacrificial layer with potassium hydroxide, forming a germanium disk on top of a silicon pedestal [Fig. 1(a)]. For these microresonators with high index contrast and large thickness, numerous transverse electric (TE) and transverse magnetic whispering gallery modes (WGMs) were found from finite-difference time-domain simulations. A particular TE WGM at 1552 nm with a cavity Q in excess of 10^5 (neglecting material absorption) is shown in Fig. 1(a).

The germanium microdisk cavities were first characterized in transmission using a side-coupled fiber taper of approximately 1 μm in diameter[9] [Fig. 1(b)]. The transmission spectrum for a 3.6 μm diameter intrinsic microdisk is shown in Fig. 1(c). Clear WGMs are seen for wavelengths longer than 1550 nm, with modes becoming increasingly sharp below the direct gap absorption edge of 1600 nm. Germanium's indirect bandgap absorption limits these Q values to a few thousand, while the direct bandgap is heavily absorbing

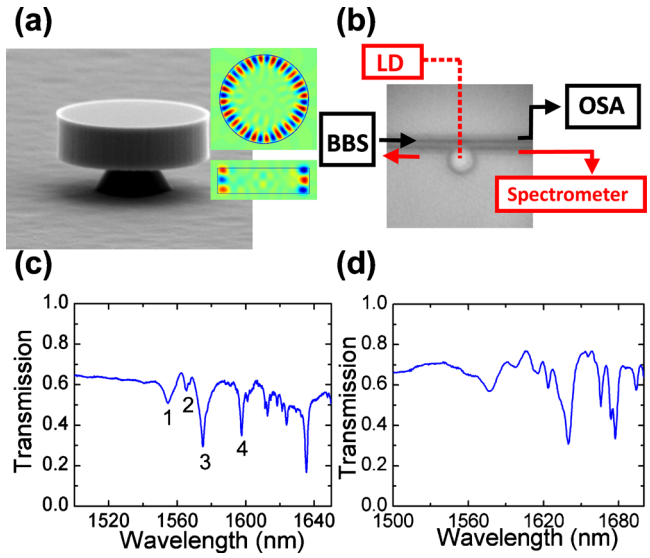

FIG. 1. (Color online) (a) SEM image of a fabricated germanium microdisk with diameter of 3.6 μm. The scale bar is 1 μm and the H_z field profile (in the direction of pedestal) of a simulated WGM (at 1552 nm) is shown to the right in both top and cross section slices. (b) Experimental setup for fiber taper probing the microdisks in both transmission (BBS to OSA path) and photoluminescence (LD to spectrometer path). LD is laser diode, BBS is broadband source, and OSA is optical spectrum analyzer. The underlying picture is an optical microscope image of the fiber taper positioned right next to the microdisk. (c) Transmission spectrum for an undoped 3.6 μm diameter germanium microdisk with four labeled WGMs. (d) Transmission spectrum for a 1×10^{19} cm^{-3} n-type disk of the same diameter.

a)Electronic mail: gshambat@stanford.edu.

and no modes are expected far past the direct band edge (wavelengths below ~1550 nm). Four modes in the transition region between minimal and heavy direct gap absorption are labeled in Fig. 1(c). In Fig. 1(d), the transmission spectrum for an n-type germanium cavity with a 3.6 μm diameter shows similar behavior as intrinsic Ge; however, due to increased free-carrier absorption (FCA), the cavity modes have lower Q.

Theoretically we expect material gain to occur for 0.2% tensile strained germanium when the nominal electron concentration approaches $\sim 10^{20}$ cm^{-3}, which can include contributions from dopant ions as well as injected carriers.[4] To find the steady-state carrier injection for a given pumping strength and initial doping level we use the rate

$$\frac{d(\Delta N)}{dt} = G - \frac{\Delta N}{\tau_{NR}} - R_\Gamma \Delta P(x_\Gamma \Delta N) - C_N(\Delta N + N_0)(\Delta N + N_0)\Delta P - C_P(\Delta N + N_0)\Delta P \Delta P. \quad (1)$$

Here ΔN and ΔP are the injected electron and hole concentrations, G is the carrier generation rate, τ_{NR} is the nonradiative recombination time estimated as 100 ns, $R_\Gamma = 1.3 \times 10^{-10}$ cm^3 s^{-1} is the direct gap recombination rate,[4] x_Γ is the fraction of electrons in the direct bandgap calculated based on Fermi–Dirac statistics, $C_N = 3 \times 10^{-32}$ cm^6 s^{-1} and $C_P = 7 \times 10^{-32}$ cm^6 s^{-1} are the electron and hole Auger recombination rates,[4] and N_0 is the n-type doping level. As an estimate, if 100 mW of 980 nm pump with a spot size of 3×3 μm^2 is fully absorbed in a 1 μm thick Ge disk that is undoped, we find $\Delta N = 8 \times 10^{19}$ cm^{-3} from the steady-state solution to the equation. Meanwhile, a sample that is doped only to 1×10^{19} cm^{-3} will have a steady-state $\Delta N = 7.5 \times 10^{19}$ cm^{-3}, for a combined electron level of 8.5×10^{19} cm^{-3}. Therefore, because the majority of band filling comes from optical injection and since the cavity modes of n-type samples are weakly visible in our detector range (which cuts off past 1600 nm), we focus our analysis on intrinsic Ge disks, although we note that similar results were obtained for n-type samples.

Optical pumping of the intrinsic germanium cavities was performed with a 980 nm laser diode through an overhead objective lens. Figure 2(a) displays the behavior of the cavity transmission for increasing continuous wave (cw) 980 nm pumping at various power levels. As the pump power increases, the band edge shifts to longer wavelengths, indicating a predominant heating effect. Meanwhile the cavity modes redshift due to the increase in refractive index caused by the bandgap reduction. In order to find the time scale by which the cavity thermally relaxes, we perform pulsed pumping by directly modulating the 980 nm laser. The laser is set to have a 50% duty cycle and the repetition rate is varied to see its effect on the microdisk transmission. When the length of the off-cycle is of the order of the thermal relaxation time, the transmission spectrum is blurred due to a superposition of cavity dips at different wavelengths, as seen in the bottom two traces of Fig. 2(b). When the off-cycle is longer than the thermal relaxation time, the transmission spectrum once again displays the cavity modes clearly as seen in the top two traces of Fig. 2(b). From the data, we find that heat dissipates on the scale of 2–5 μs for this particular size Ge microdisk.

Photoluminescence from the germanium cavity was collected by feeding one pigtail of the fiber taper into a spectrometer, where it was detected by a cooled InGaAs detector array. In Fig. 3(a), we see that the output spectrum for 750 μW of 980 nm pump power consists of a small background Ge PL as well as four cavity-enhanced peaks, corresponding exactly to the four peaks found in transmission. From this result, we see that germanium microdisk cavities on silicon substrates can indeed emit resonant PL near 1.55 μm. Emission is possible before the onset of lasing because these cavity modes are positioned at the edge of the direct gap, where absorption is still low and resonant modes can be sustained. We attribute the PL to the direct gap transition due to the similarity of emission properties compared to previous studies.[5] The two narrow peaks labeled 2 and 3 in Fig. 3(a) are located at 1565 and 1575 nm, respectively, and have intrinsic taper-loaded Q-factors of 700 and 530 (as

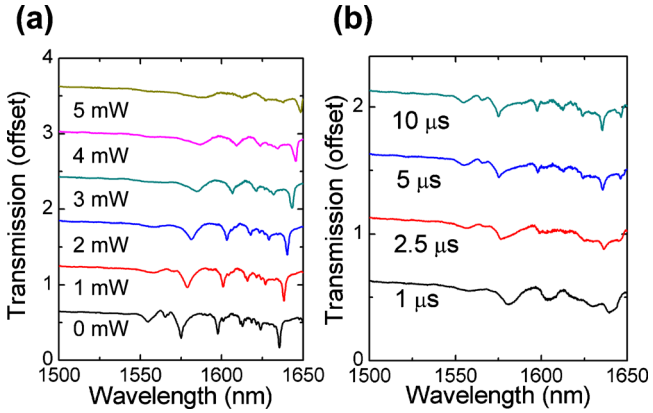

FIG. 2. (Color online) (a) Transmission spectrum for the undoped 3.6 μm diameter disk under cw 980 nm laser pumping. A broadband source coupled to fiber taper is used to probe the cavity in transmission, while optical pumping is performed with a cw 980 nm laser in the direction perpendicular to the chip. Spectra are offset by 0.6 units for clarity. (b) Transmission spectra of the same disk under 50% duty cycle pulsed pumping with 5 mW peak power of the 980 nm laser. Legend labels indicate off-cycle duration and spectra are offset by 0.5 units.

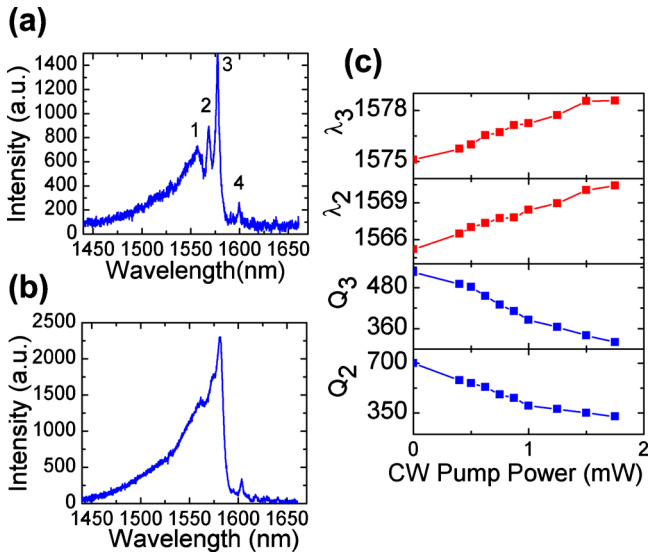

FIG. 3. (Color online) (a) PL spectrum of the germanium microdisk for a 750 μW cw pump at 980 nm. Peaks labeled 2 and 3 are the main emission peaks analyzed. (b) PL spectrum under 2 mW of cw pump power. (c) Cavity mode wavelength and quality factor behavior for modes 2 and 3 vs increasing cw pump power. The zero pump power data point is taken from transmission measurements.

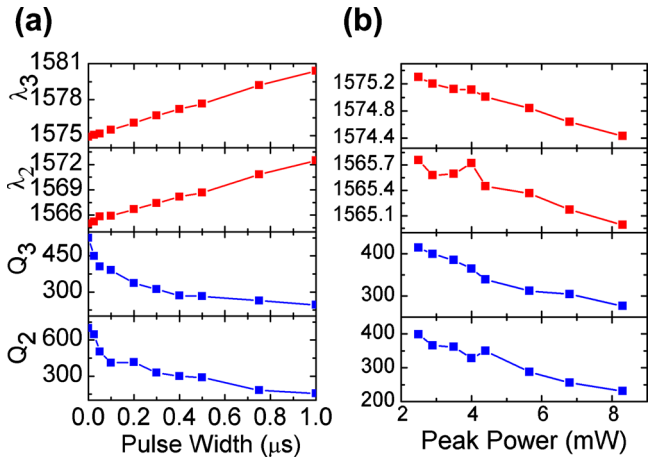

FIG. 4. (Color online) (a) Quality factor and wavelength behavior of cavity modes 2 and 3 vs the on-pulse width for a 1 μs repetition period. (b) Q-factor and wavelength behavior for the same modes as the peak power is increased for a 50 ns on-pulse and a 1 μs repetition period.

measured in transmission) due to the background germanium absorption. As we increase the pump power, we monitor the change in quality factor and wavelength position of these two modes as seen in Fig. 3(c). For both modes, the Q-factor decreases with increasing power and the wavelength redshifts, in agreement with the transmission spectra. Figure 3(b) shows a PL spectrum under 2 mW pump power, confirming this trend.

To reduce the impact of heating, we perform pulsed pumping measurements with the directly modulated 980 nm laser. Figure 4(a) shows the effect of reducing the duty cycle of the pump for a 1 MHz repetition rate and a peak power of 5 mW. As the duty cycle is decreased from 100% to 2.5%, the Q-factor of the cavity modes increases and the wavelength decreases, approaching the unpumped value. Therefore we conclude that pulsed pumping is an effective way of reducing the parasitic heating. Next, we set the repetition rate at 1 MHz and the pulse width at 50 ns and increase the peak power [Fig. 4(b)]. Significant linewidth narrowing or material transparency did not take place for these pumping conditions. Instead, increasing peak power leads to a measured Q reduction as well as a blueshift of the cavity modes, even beyond the intrinsic values. Likely, the measured blueshift and Q-factor reduction are a result of FCA dominating over material gain. Although our pump laser is powerful enough to reach the injection levels needed for inversion, as calculated above, the cavity modes broaden completely before that level can be reached, suggesting that the FCA is too high for low or undoped samples.

In summary, optically pumped germanium microcavities on silicon were investigated as emitters for on-chip source applications. Clear cavity WGMs were collected via fiber taper and analyzed under various pump conditions. Transmission and PL measurements revealed that heating is a main detriment in preventing lasing by reducing the material gain. The high pumping conditions necessary to invert germanium are a direct result of the inability to heavily dope epitaxially grown Ge-on-Si to the desired $\sim 10^{20}$ cm^{-1}. Although aggressive pumping conditions such as Q-switched lasers can be used to overcome this hurdle,[8] a more practical method must be developed for real applications. With current progress in codoped ion implantation techniques, n-type doping levels in excess of 10^{20} cm^{-3} have been demonstrated.[10] We believe that such high doping may be possible to implement in germanium microcavities, thereby relaxing the pumping conditions, optical or electrical, needed for lasing to occur.

Financial support for this work was provided by the Stanford Graduate Fellowships and the NSF GRFP. S-L.C. would also like to acknowledge the support of the ABB Fellowship Fund. The authors acknowledge the support of the Interconnect Focus Center, one of six research centers funded under the Focus Center Research Program (FCRP), a Semiconductor Research Corporation entity. This work was performed in part at the Stanford Nanofabrication Facility of NNIN supported by the National Science Foundation under Grant No. ECS-9731293.

[1] P. H. Lim, S. Park, Y. Ishikawa, and K. Wada, Opt. Express **17**, 16358 (2009).
[2] J. Menéndez and J. Kouvetakis, Appl. Phys. Lett. **85**, 1175 (2004).
[3] J. Xia, Y. Takeda, N. Usami, T. Maruizumi, and Y. Shiraki, Opt. Express **18**, 13945 (2010).
[4] J. Liu, X. Sun, D. Pan, X. Wang, L. C. Kimerling, T. L. Koch, and J. Michel, Opt. Express **15**, 11272 (2007).
[5] S.-L. Cheng, J. Lu, G. Shambat, H.-Y. Yu, K. Saraswat, J. Vuckovic, and Y. Nishi, Opt. Express **17**, 10019 (2009).
[6] X. Sun, J. Liu, L. C. Kimerling, and J. Michel, Opt. Lett. **34**, 1198 (2009).
[7] T.-H. Cheng, C.-Y. Ko, C.-Y. Chen, K.-L. Peng, G.-L. Luo, C. W. Liu, and H.-H. Tseng, Appl. Phys. Lett. **96**, 091105 (2010).
[8] J. Liu, X. Sun, R. Camacho-Aguilera, L. C. Kimerling, and J. Michel, Opt. Lett. **35**, 679 (2010).
[9] G. Shambat, Y. Gong, J. Lu, S. Yerci, R. Li, L. D. Negro, and J. Vuckovic, Opt. Express **18**, 5964 (2010).
[10] J. Kim, S. W. Bedell, S. L. Maurer, R. Loesing, and D. K. Sadana, Electrochem. Solid-State Lett. **13**, H12 (2010).